Challenges in Roll-Sway Motion Cueing Fidelity: A view from academia

Steven J. Hodge
Visiting Research Fellow

Sylvain Manso
Visiting Research Fellow

Mark D. White
Simulation Laboratory Manager

The University of Liverpool
Liverpool, UK

Abstract

This paper describes an experiment conducted to investigate the effects of roll-sway motion cueing algorithms on perceived simulator motion fidelity in a lateral repositioning task. The aims of the investigation were split into two primary objectives. Firstly, to repeat a previous roll-sway experiment conducted on the same simulator facility with the same aircraft model and motion drive algorithm, but with a different pilot, to determine if the results were repeatable. Secondly, to introduce an alternative motion drive algorithm. In the original roll-sway investigation the classical washout algorithm was used throughout the experiment. During the current experiment a comparison was made between the classical washout algorithm and the recently developed Lateral Manoeuvring Motion algorithm. The findings of the current experiment are in remarkably good agreement with those of the previous roll-sway experiment, particularly in terms of pilots' subjective impressions of simulator fidelity. The results confirm that the roll-axis motion-filter break frequency has a strong influence on perceived motion fidelity, at the two break-frequencies tested in both experiments and at an intermediate break frequency tested in this experiment. Pilot opinion of the motion cues provided by the Lateral Manoeuvring Motion algorithm were very positive, although the trends in subjective and objective measures, observed while changing the motion filter coefficients, were not as clear or compelling as they were for the classical washout scheme. To the authors' knowledge this is the first time that the Lateral Manoeuvring Motion algorithm has been systematically tested for a helicopter roll-sway task on a short-stroke motion platform.

Notation

$\mathbf{a}$	linear acceleration vector, m/s^2
$\mathbf{f}$	specific force vector, m/s^2
$\mathbf{g}$	gravity vector [0 0 g], where g = 9.81m/s^2
f_y	lateral specific force, m/s^2
HP	high-pass filter
K	motion filter gain, non-dimensional
L_p	normalised vehicle roll damping derivative, 1/s
L_δ	lateral cyclic sensitivity derivative, rad/s^2/inch
p	vehicle roll rate, rad/s
p_c	simulator roll rate, rad/s
r_z	position of pilot vestibular centre with respect to the simulator rotational centre, m
s	Laplace operator
v	vehicle body-axis lateral velocity, m/s
y	vehicle earth-axis lateral position, m
y_c	simulator lateral displacement, m
δ_{lat}	lateral cyclic position, inches
ϕ	vehicle roll angle, rad
ϕ_c	simulator roll angle, rad
ω_b	first-order high-pass break frequency, rad/s
ω_{hp}	second-order high-pass break frequency, rad/s
ζ_{hp}	second-order damping ratio, non-dimensional

Presented at the Royal Aeronautical Society Flight Simulation Group Conference on *'Challenges in Flight Simulation'*, 9-10 June 2015, London, UK.

Introduction

The challenge that flight simulator operators and designers frequently face is that of providing high-fidelity vestibular motion cues in the roll-sway axes. Examples of fixed-wing aircraft manoeuvres which are sensitive to roll-sway motion fidelity include coordinated turns and ground taxiing. A coordinated turn is a basic flight manoeuvre whereby the dynamics of the aircraft are fully coordinated. The term 'fully coordinated' in this sense means that the acceleration vector, experienced by the pilot, remains aligned through the vertical axis of the pilot (i.e. the pilot does not 'feel' any lateral acceleration during the manoeuvre). A similar manoeuvre performed by rotary-wing aircraft is the lateral translation in hovering flight. Figure 1 shows a schematic of a helicopter in a fully coordinated lateral translation. Some commonly cited pilot criticisms of motion cueing during coordinated roll-lateral manoeuvres are summarised in Refs. 1-3. In Ref. 1 spurious sway motion cues are characterised as being '*out of phase*' or '*like a student* [pilot] *on the rudder pedals*', in Ref. 2 they are referred to as a '*reverse side force*' and a reduction in amplitude of the platform roll motion is suggested as a possible cure. In Ref. 3 spurious lateral motion cues are described as '*the leans*'.

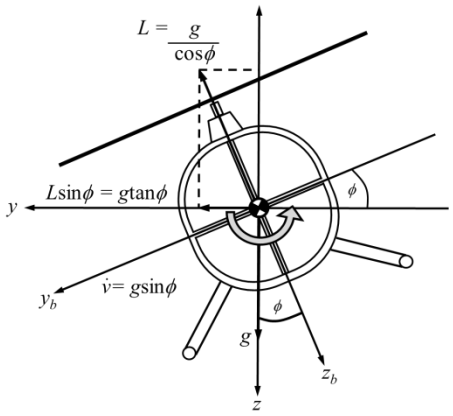

Figure 1. Helicopter in a coordinated lateral translation

To illustrate the source of these objections we can examine the simple case of a pilot step input in the roll-axis. In this example an aircraft model is used with the equations of motion given in Equations (1) and (2).

$$\ddot{\phi} = L_p\dot{\phi} + L_\delta\delta_{lat} \qquad \ldots(1)$$

$$\dot{v} = g\sin\phi \qquad \ldots(2)$$

where δ_{lat} is the pilot's lateral stick input and the coefficients L_p and L_δ are, respectively, the aircraft roll damping and the lateral control sensitivity. Figure 2 shows the response of such an aircraft model to a step input in δ_{lat} at 1 second. It is assumed that the distance between the pilot's seat and the aircraft centre of gravity is small. The final plot in Fig. 2 is the lateral specific force experienced at the pilot's head. In flight, as in a simulator, pilots sense body motion largely through their vestibular system, which consists of two important sensors, both located in the inner ear – the semicircular canals and the otoliths. The semicircular canals sense angular accelerations in the roll, pitch and yaw axes; and the otoliths detect the specific force acting on the head in the longitudinal, lateral and vertical directions. Specific force at the centre of gravity (c.g.) of a vehicle is defined as the sum of the vehicle's external forces (including gravity)

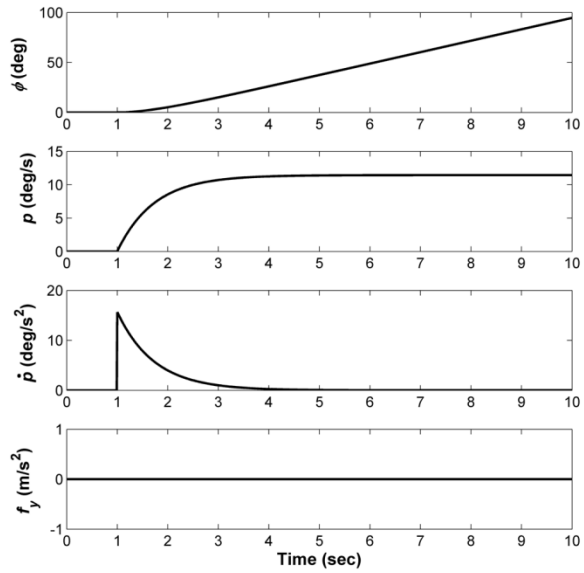

Figure 2. Aircraft model response to a step input

divided by the vehicle mass less the gravitational component (Equation (3)). This means that for an aircraft, the specific force at the c.g. is the sum of all aerodynamic and ground reaction forces.

$$\mathbf{f} = \mathbf{a} - \mathbf{g} \qquad \ldots(3)$$

It can be seen from Fig. 2 that in the aircraft the pilot will sense no lateral specific force, as previously discussed, because in this case, $f_y = \dot{v} - g\sin\phi$, which is equal to zero. However, if the same manoeuvre where performed in a flight simulator (Fig. 3) then the specific force experienced by the pilot would be given by

$$f_y = \ddot{y}_c - r_z\ddot{\phi}_c - g\sin\phi_c \qquad \ldots(4)$$

The first term on the right-hand side of Equation (4) is the lateral acceleration of the motion platform's centre of rotation (or centroid). This is a desired motion cue generated by pure translation of the platform. The remaining terms are undesirable side-effects or 'false cues', with the second term being the lateral acceleration at the pilot's vestibular centre (assumed to be half way between the pilot's ears) induced by platform rotation and the final term being caused by orientation of the gravity vector.

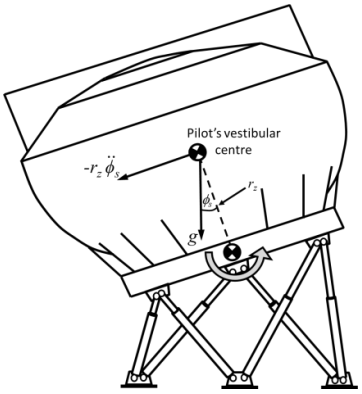

Figure 3. Flight simulator motion platform in a lateral translation

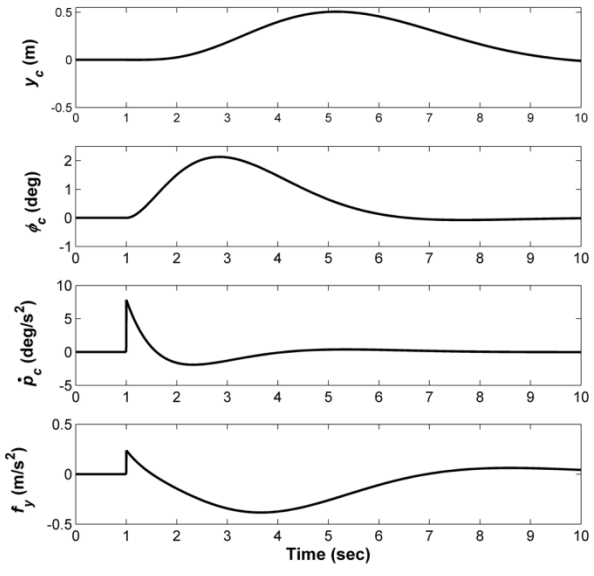

Figure 4. Motion platform response to step input

The response of the motion platform to the aircraft model step input (Fig. 2) is shown in Fig. 4. It can be seen that the simulator response in the roll-axis is scaled and also 'washed-out' back to zero, compared to the aircraft (Fig. 2). This is the effect of the so-called washout filters in the motion drive algorithm. These will be discussed in detail later. The lateral specific force, sensed at the pilot station, is shown at the bottom of Fig. 4. The initial spike in f_y is caused by the rotational acceleration of the simulator cabin with the pilot situated above the simulator's rotational centre (the $-r_z\ddot{\phi}_c$ term in Equation(4)). The remainder of the specific force is mainly due to gravity vector alignment (the $-g\sin\phi_c$ term in Equation(4)). Hence, the lateral specific force experienced by the pilot in the simulator, will be significantly different to that which would be experienced in the aircraft. This constitutes a significant false cue, which should be compensated for in the simulator's motion drive algorithm. Of the two 'false' cues it is the longer term component ($-g\sin\phi_c$) which is the source of complaints regarding the spurious "out of phase" or "leaning" motion cues. The transient component ($-r_z\ddot{\phi}_c$) could, if unchecked, lead to pilot-simulator biodynamic coupling.

The purpose of this paper is to report on an experiment to investigate the effects of two different roll-sway motion cueing algorithms, which attempt to reduce the effects of these false cues in different ways. The two chosen algorithms are the classical washout and the Lateral Manoeuvring Motion (Lm^2) algorithms. The next section gives the background to the current experiment in more detail by presenting results from several previous experiments. After this the two motion drive algorithms are discussed in detail, including a short parametric study. The experimental set-up is then described before the results of the experiment are presented and explained. The paper draws to an end with a discussion of the main conclusions and recommendations for further work.

Background

Overview

A simplified overview of the manual control loop comprised by the pilot, the helicopter simulation and motion drive algorithm is shown in Fig. 5. In the roll-sway axes the pilot provides control commands, δ_{lat}, by means of lateral cyclic stick inputs, which results in a roll angle, ϕ, being generated by the aircraft model dynamics (Equation (1)). The roll angle is the input signal for the lateral dynamics (Equation (2)), resulting in a lateral aircraft displacement, y. The aircraft roll angle, ϕ, and lateral position, y, are perceived by the pilot through the simulator visual system at full-scale. Simultaneously, the roll angle is input into the motion drive algorithm (in the form of roll acceleration), which computes the roll angle, ϕ_c, and lateral position, y_c, drives to the motion platform. Compared to the visual cues these signals will be scaled and filtered. This is usually accomplished by passing the drive signals through so-called 'washout' filters.

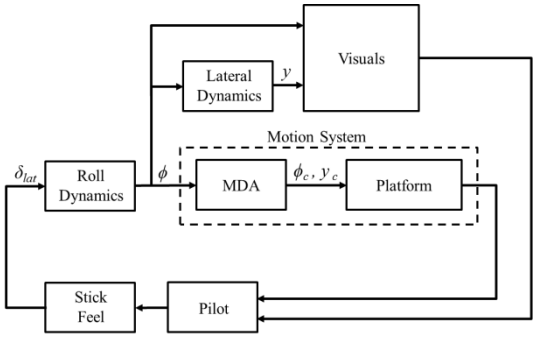

Figure 5. Overview of flight simulator control loop

The choice of washout filter is largely dependent on the simulator application. For example, Reid and Nahon[4] found low-order, such as first- and second-order, filters were generally sufficient for the simulation of large transport aircraft. In other applications, which required more dynamic manoeuvres on short-stroke motion platforms, third-order filters are often preferred. The transfer function for a third-order filter can be written by cascading first- and second-order filters, so that a third-order roll-axis washout filter is given by Equation (5).

$$K_\phi HP_\phi(s)=K_\phi\left(\frac{s^2}{s^2+2\zeta_{hp\phi}\omega_{hp\phi}s+\omega_{hp\phi}^2}\right)\left(\frac{s}{s+\omega_{b\phi}}\right) \qquad \ldots(5)$$

where $\zeta_{hp\phi}$ and $\omega_{hp\phi}$ are, respectively, the damping ratio and break-frequency of the second-order filter, and $\omega_{b\phi}$ is the break frequency of the first-order filter. An addition high-frequency gain or scaling factor, K_ϕ, is applied at the input to the filter. The values of these coefficients must be carefully selected to provide 'good' motion cues over a range of frequencies, whilst at the same time constraining the platform's excursions within the devices achievable envelope.

Early Research

Several researchers have examined various roll-sway tasks to determine the requirements for 'good' motion cues in the roll-sway axes. Stapleford *et al.*[5] examined a roll control experiment for a vertical take-off and landing (VTOL) vehicle hovering in gusty air, using a six degree-of-freedom motion base. In Stapleford's experiments, pilots were instructed to minimise roll deviations using cues from the motion platform and from a horizon display showing roll angle. A first-order washout filter was used in the roll-axis with a second-order filter in the sway-axis. Stapleford concluded that for manual tracking tasks the translational (sway) motion cues appeared to be less important than rotational motion cues. According to Stapleford, pilots were unaware of motion washout in the roll-axis when the break frequency, $\omega_{b\phi}$, was 0.5 rad/s and increasing it to 2 rad/s had only a minor effect.

A study by Jex *et al.*[6] investigated pilot performance during target tracking and disturbance rejection. This experiment examined motion cues in the roll-axis only, but the motion system could be configured so that pilots rolled the simulator either sitting upright or lying on their backs. The first case represents the normal situation where false cues, caused by orientation of the gravity vector, would be present. The second case presents no such false cues. Jex examined several cases including full-motion, no-motion, scaled-motion and various first- and second-order washout filters. The study found that using scaled motion or first-order washout filters produced similar improvements in pilot performance, but the preferred washout filter was a first-order filter with a high-frequency gain of between 0.5 and 0.7 and a break frequency, $\omega_{b\phi}$, of 0.3 to 0.5 rad/s. Jex also discovered that pilots used false tilt cues, experienced during upright rolling, to improve their tracking performance, even though the resulting lateral specific force was generally less than 0.1g; the performance improvement was small but the use of false cues by pilots has significant implications for training simulators.

Bray[7] carried out initial experiments on a motion simulator capable of large lateral displacements (±50ft) and roll angles (±45º) to investigate the handling qualities of large transport aircraft. As part of these experiments Bray conducted a limited exploration aimed at developing general motion cueing requirements for flight simulators. These tests involved constraining the motion of the simulator using second-order washout filters and scaling the motion drive signals. Bray found that with a roll-axis gain of unity and a break frequency, $\omega_{hp\phi}$, of 0.5 rad/s, pilots reported slight contradictions between visual and motion cues. Increasing the break frequency to 1.0 rad/s significantly degraded the pilots' ability to stabilise the Dutch-roll mode. Reducing the roll-axis motion gain to 0.5 reduced the phase-related contradictions, described above, and halved the platform's sway-axis excursions, also reducing the distracting mechanical noise generated by the motion system's mechanisms. A general conclusion from Ref. 7 is that, for large transport aircraft, cockpit sway motion cues appear to be more important than roll motion cues.

In Europe, van Gool[8] used a four degree-of-freedom motion platform (with no sway motion) to investigate the influence of motion drive algorithms, in the pitch and roll axes, on pilot performance while stabilising an aircraft in turbulence. Second-order washout filters were used with only the break frequency being varied; filter gain and damping ratio remained fixed at unity. The results concluded that no significant differences in pilot performance, or subjective feedback, could be observed when the break frequency, $\omega_{hp\phi}$, was varied from 0.1 to 0.5 rad/s.

Bergeron[9] and Shirachi and Shirley[10] both examined the effects of scaling the roll-sway motion cues with a gain between zero and unity, during a tracking task and a disturbance rejection task. For a tracking task Bergeron[9] found that pilot performance degraded with motion gains of less than 0.25. However, in their disturbance rejection task Shirachi and Shirley[10] found pilot performance was similar to the no motion case when the roll-axis motion gains were reduced below 0.5.

In a follow-on to his earlier study, summarised in Ref. 1, Jex investigated the effects of various second-order washout configurations using a motion platform with ±10ft of lateral travel. A fidelity criteria was proposed, based on pilots' subjective impressions of the motion cues, defining acceptable combinations of gain and break frequency for the sway-axis. The proposed criteria are shown in Fig. 6, where the region of uncertainty is due to the limited number of test points considered. However, pilot opinion was not always consistent and changed depending on the nature of the task (e.g. sidestep or target tracking), besides which, changes in the motion cues caused by varying the washout filter coefficients were deemed very subtle, making it difficult for pilots to provide subjective feedback. In general, results showed that pilot objections increased when the amplitude of the false sway cues was greater than 0.1g.

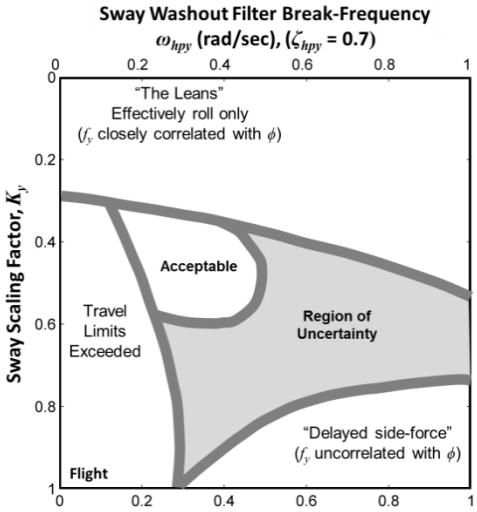

Figure 6. Jex's sway axis motion fidelity criteria

In Ref. 11, Sinacori used a large motion platform to investigate an 'S'-turn manoeuvre along a runway at 60kts with a six-degree-of-freedom model of a high performance helicopter. Sinacori found that an acceptable simulation was maintain with a sway filter gain of 0.6, while values of 0.4 or less elicited pilot objections, because of anomalous side-forces. In addition Sinacori proposed further motion fidelity criteria based on measures of the gain and phase shift between the aircraft model output and the motion system commands at a frequency of 1 rad/s. Figure 7 presents Sinacori's rotational and translational criteria and the 3-point rating scale used by Sinacori to elicit pilot opinion (the rotational criteria also includes a summary of the roll-axis results reviewed so far). In Ref. 11 Sinacori acknowledges that these criteria '*have little or no support other than intuition*'. Nevertheless, they remain the most complete and coherent set of motion fidelity criteria available today.

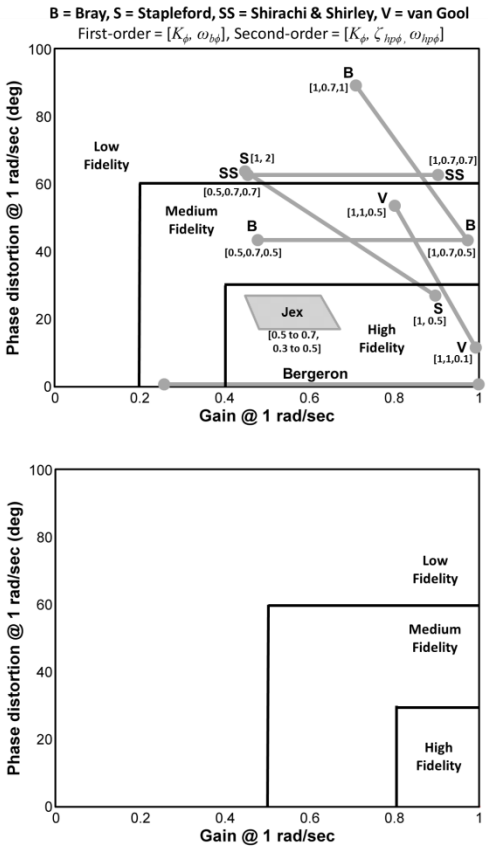

High	Motion sensations are close to those of visual flight
Medium	Motion sensation differences are noticable but not objectionable
Low	Differences are noticable and objectionable, loss of performance, disorientation

Figure 7. Sinacori's rotational and translational criteria

Recent Research

In Ref. 3 Schroeder investigated a 20ft sidestep task with a coordinated helicopter model on the NASA Ames Vertical Motion Simulator (VMS), which is capable of ±20ft of lateral travel. Motion platform commands were scaled from zero (no-motion) to unity (full-motion) in both the roll and sway axes, with no washout filters applied. Roll and sway motion gain variations were found to have a significant effect on pilots' perceptions of motion fidelity, but not on their positioning performance; although control activity (workload) did decrease as the motion gains increased. Pilot opinion of the full-motion case was less positive than expected, due to distracting mechanical noise generated by the motion system. The no-motion case consistently received poor fidelity ratings. Schroeder's experiment has subsequently been repeated by a number of researchers.

Mikula *et al.*[12] investigated the same task with the same aircraft model, again using the NASA VMS, but this time with second-order roll and sway washout filters. The results of this study suggested that motion fidelity was strongly dependent on the roll motion phase distortion, the lateral motion phase distortion and lateral motion gain. Pilots' opinion of motion fidelity improved when the roll and sway filter break-frequencies, $\omega_{hp\phi}$ and ω_{hpy}, were small and the lateral motion gain was high. A high break frequency in the roll-axis, however, always resulted in poor motion fidelity, regardless of the other parameters.

In Ref 13, Chung *et al.* performed a similar experiment to Schroeder, this time on an 80 inch stroke hexapod simulator, again using the same task and model. Chung investigated three fidelity levels for roll motion (low, medium and high) taken from the Sinacori criteria[11] and four sway motion filters with increasing phase distortion. In order to achieve the fidelity levels, in the roll-axis, filter gain and break frequency where changed together. In the sway-axis only break frequency was altered and gain remained fixed at unity. The simulator often ran out of lateral travel while testing high-fidelity roll configurations with sway filters that provided low phase distortion, leading to less favourable subjective ratings than expected. Two high-fidelity roll configurations were successfully tested with lateral filters giving higher phase distortions and were awarded poor fidelity ratings. The low fidelity roll-axis configurations were awarded poor fidelity ratings regardless of the sway-axis filter settings.

In Ref. 14 Wiskemann *et al.* also repeated Schroeder's experiment this time with an anthropomorphic robot arm simulator mounted on a lateral track. This experiment investigated a hybrid of the motion drive algorithms used by Schroeder[3] and Mikula[12]/Chung[13] by using a second-order filter in the roll-axis and a scaling factor in the sway-axis. The results of this experiment showed that perceived fidelity was generally better when the roll and sway motion gains were high. However, the roll-axis break frequency, $\omega_{hp\phi}$, had the most pronounced effect on both subjective and objective measures; the subjective ratings being consistently worse for conditions with stronger roll washout (i.e. higher break-frequency). The conclusions of Ref. 14 suggests that reducing the roll and lateral motion gains is a more effective means of attenuating simulated motion than increasing the roll washout, since perceived motion fidelity appears to be less sensitive to roll and sway gain than to roll washout.

Finally, Hodge *et al.*[15] used a short-stroke hexapod simulator with a similar task and aircraft model to investigate optimising the cues for third-order filters in the roll and sway axes. To elicit pilot opinion a new 10-point motion fidelity rating scale was devised, since they considered the existing three point scale to be too coarse to measure subtle differences in motion cues. In their experiment Hodge *et al*. found good motion cues could only be obtained by careful selection of the roll and sway-axis motion gains. Selecting a sway-axis gain which was too low and a roll-axis gain which was too high, resulted in 'harsh' motion cues. Increasing the sway gain improved pilot opinion, but it was difficult to use the full platform sway performance due to audible noise. Like Mikula[12] and Wiskemann[14] they also found that roll-axis break frequency had a dominant effect on motion fidelity. Reference 15 reports that with a high break frequency in the roll-axis, leading to mismatch (phase shift) between the visual and vestibular cues, the only way to improve pilot opinion was to reduce the roll-axis motion gain, effectively 'masking' the cause of pilot objections.

Motion Drive Algorithms

Classical Washout Algorithm

The classical washout scheme has been in existence for several decades and has been widely used as the basis for the motion drive programs employed in many simulators in operation around the world today[16,17]. This means that most pilot training is conducted on simulators which employ the classical washout algorithm in some form. Figure 8 shows a schematic of the elements of the classical washout algorithm which are used to generate roll and sway motions in response to aircraft roll motion.

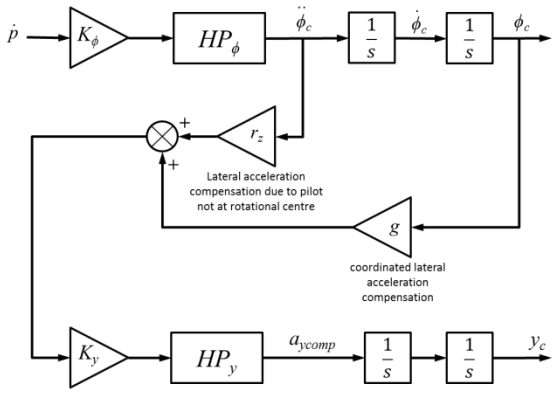

Figure 8. Classical washout algorithm

For a pure roll input the platform roll motion is the desired response and lateral motion is used to properly coordinate the cockpit motion. The high-pass filters, HP_ϕ and HP_y, are generally implemented using second or third-order filters (see Equation (5)). The time history of the classical washout response to a pilot step input in lateral stick, δ_{lat}, was shown in Fig. 4. The resulting lateral specific force experienced by the pilot is given in Equation (4) were the platform lateral acceleration command can be written as

$$\begin{aligned} \ddot{y}_c = a_{ycomp} &= K_y HP_y\left(r_z\ddot{\phi}_c + g\phi_c\right) \\ &= K_y HP_y\left(r_z K_\phi HP_\phi\ddot{\phi} + gK_\phi HP_\phi\phi\right) \end{aligned} \quad \ldots(6)$$

Substituting Equation (6) back into (4) and using small angle approximations

$$\begin{aligned} f_y = K_y HP_y\left(r_z K_\phi HP_\phi\ddot{\phi} + gK_\phi HP_\phi\phi\right) \\ - r_z K_\phi HP_\phi\ddot{\phi} - gK_\phi HP_\phi\phi \end{aligned} \quad \ldots(7)$$

Finally, re-arranging Equation (7) gives

$$\begin{aligned} f_y = r_z K_\phi HP_\phi\ddot{\phi}\left(K_y HP_y - 1\right) \\ + gK_\phi HP_\phi\phi\left(K_y HP_y - 1\right) \end{aligned} \quad \ldots(8)$$

From the previous discussion it is clear that the lateral specific force, f_y, should, ideally, be zero. It can be seen from Equation (8) that false sway cues will be reduced and, therefore, simulation fidelity increased, when the gain of the sway filter, $K_y HP_y$, is close to unity. Alternatively, a reduction in the roll-axis motion gain, $K_\phi HP_\phi$ will also bring about a reduction in false sway cues, but at the expense of fidelity in the roll channel.

Lateral Manoeuvring Motion Algorithm*

The Lateral Manoeuvring Motion or Lm^2 algorithm introduces a modification to the conventional classical washout scheme (Fig. 9). The motivation for developing Lm^2 is the generally poor perception of motion cues, by pilots, during lateral manoeuvres[18]. The modifications embodied in Lm^2 are designed to significantly reduce the false sway cues experienced by the pilot during lateral manoeuvring (e.g. coordinated turns and ground taxiing). However, in order to accomplish these improvements some fidelity in the roll-axis has been sacrificed. The Lm^2 algorithm has been 'retro-fitted' to a number of existing flight training simulators[19] and specified as part of some new training simulators[20], and has received positive feedback from pilots.

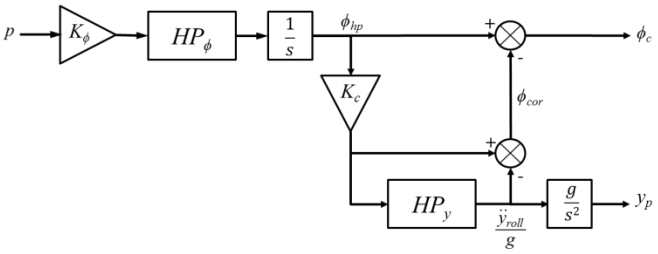

Figure 9. Lateral Manoeuvre Motion algorithm (Lm^2)

The high-pass roll filter, HP_ϕ, is implemented using a second-order filter and, the sway filter, HP_y, is normally implemented using a first-order filter. However, for platforms with a limited motion envelope, a second-order filter may be used. In the case of the Lm^2 algorithm the lateral specific force sensed by the pilot is given by

$$f_y = \ddot{y}_{roll} - g\phi_c \quad \ldots(9)$$

Where the platform roll angle is given by

$$\phi_c = \phi_{hp} - \phi_{cor} = \phi_{hp} - \left(K_c\phi_{hp} - \frac{\ddot{y}_{roll}}{g}\right) \quad \ldots(10)$$

Substituting Equation (10) into Equation (9) gives

$$f_y = \ddot{y}_{roll} - g\left(\phi_{hp} - K_c\phi_{hp} + \frac{\ddot{y}_{roll}}{g}\right) \quad \ldots(11)$$

Multiply out and simplifying Equation (11) yields

$$f_y = g\phi_{hp}(K_c - 1) = gK_\phi HP_\phi\phi(K_c - 1) \quad \ldots(12)$$

Lm^2 is a patented motion control method owned by Filip Vanbiervliet. The exclusive commercial rights are granted to Acceleration Worx bvba (AWx), Leuven, Belgium. Any and all use of the motion control method is subject to prior approval by AWx.

The primary difference between the Lm^2 and the classical washout algorithm is the feedback of, ϕ_{cor}, into the roll channel. In the Lm^2 arrangement if, K_c, the 'coordinating' gain is unity then it is easily seen that the specific force sensed by the pilot will be zero (see Equation (12)). However, it can also be seen that as the coordinating gain increases so too does the distortion in the platform roll angle compared to, ϕ_{hp}. It can be shown from Equation (10) that when, K_c, is unity the roll angle, ϕ_c, is proportional to the lateral acceleration, $\ddot{y}_{roll}/g$, which is the exact amount of roll angle required to make Equation (9) equal to zero. In other words the platform will tilt in proportion to the lateral acceleration. Values of, K_c, less than unity will decrease the lateral coordination but will also lead to less distortion in platform roll response. Note also that the inputs to the Lm^2 algorithm are the specific force and rotational rates at the pilot station rather than the motion centroid. Hence, the sway channel output, y_p, must be transformed to the commanded motion centroid displacement, y_c, using Equation (13). In contrast to the classical washout algorithm which filters the centroid signals.

$$y_c = y_p + r_z\phi_c \qquad \ldots(13)$$

The response of the Lm^2 algorithm (K_c = 0.8) to a step in lateral stick input is shown in Fig. 10 together with the classical washout response. The advantage of the Lm^2 response, compared to the classical washout, is the significant reduction in the false lateral specific force cues experienced by the pilot. The disadvantage is the reduction in platform roll angle and, that the roll angle is reversed before eventually being washed-out. A further potential disadvantage is the static offset in platform lateral position. This will be a particular issue if the Lm^2 algorithm is applied to a short-stroke motion platform with a small useable envelope.

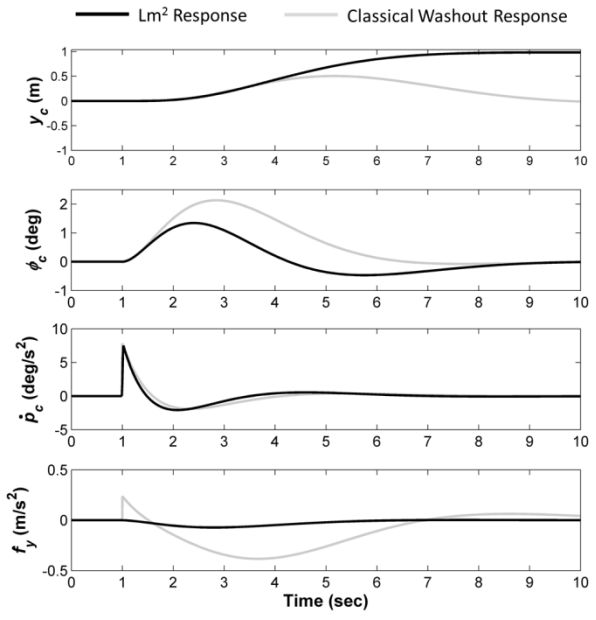

Figure 10. Lm^2 and classical washout response to step input

One method of removing this static offset is to replace the first-order sway filter, HP_y, with a second-order filter. The effect of introducing a second-order filter into the sway channel is shown in Fig. 11. It can be seen that lateral position, y_c, now returns to neutral. Importantly, the lateral specific force is still significantly reduced and the only disadvantage is a slight increase in distortion of the roll motion.

Parametric Study

Two methods of analysing the behaviour of the classical washout and Lm^2 algorithms are now presented. The first is via inspection of time histories of the responses to a pilot step input, with varying values of washout filter coefficients. The second is by calculating the frequency response. In the frequency domain two transfer functions are considered - the roll channel transfer function and the specific force error to roll input transfer function.

Classical Washout:

Figure 12 shows the roll acceleration and displacement response of the classical washout algorithm using second and third-order filters (Equation (5)), with varying break frequency, $\omega_{hp\phi}$, and with the gain, K_ϕ, set to unity. It can be seen from Fig. 12b that as the break frequency is reduced the filter output increasingly resembles the aircraft model roll acceleration. The roll displacement is washed-out compared to the aircraft roll angle (Fig. 12a), but with a low break frequency the platform roll motion will achieve a larger peak angle and will be of longer duration compared to smaller break-frequencies. It can also be seen that for 3rd order filters the roll motion is slightly distorted, with a reversal in direction during the washout phase, compared to the 2nd order response. Changing the gain, K_ϕ, would simply scale the responses shown in Fig. 12.

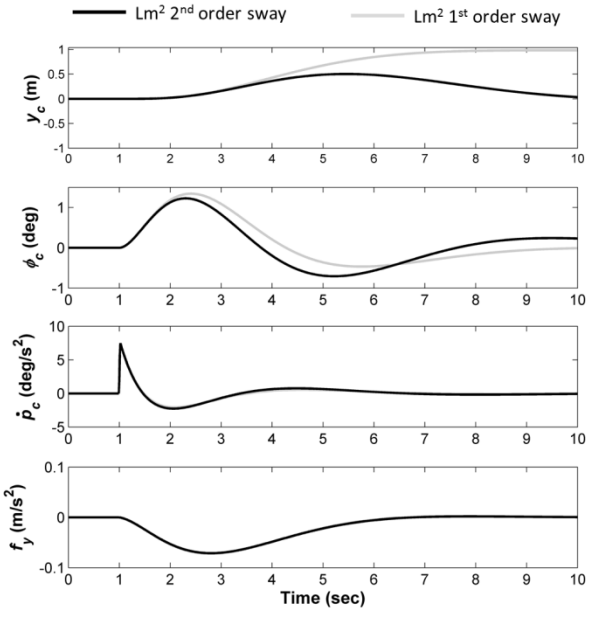

Figure 11. Lm^2 response to step input (with 1st and 2nd order sway-axis filters)

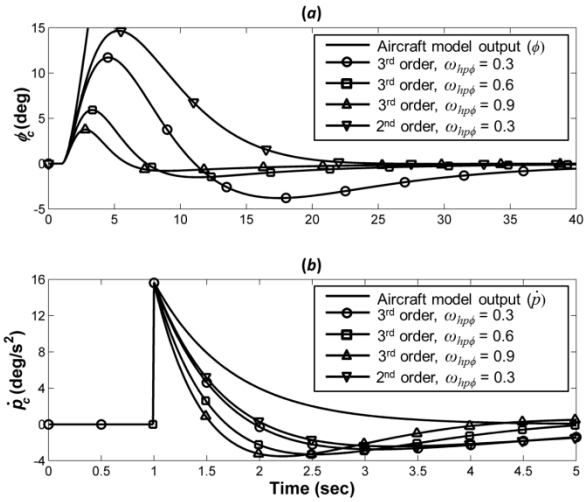

Figure. 12 Classical washout roll response

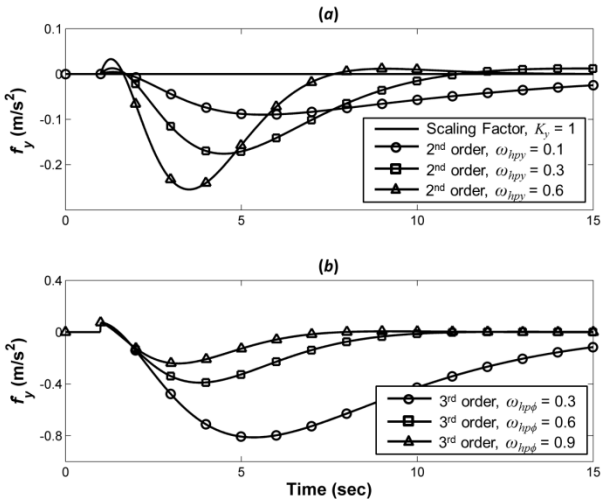

Figure 13. Classical washout lateral specific force

The lateral specific force experienced by the pilot is shown in Fig. 13. Figure 13a shows the specific force produced using second-order sway-axis filters with varying break frequency, ω_{hpy}, compared to a simple scaling factor (i.e. removing the sway-axis filter, HP_y) of, K_y, equal to unity. In the case were a scaling factor is used it can be seen from Equation (8) and Fig. 13a that zero specific force, or full coordination, is achieved when K_y is unity. In the three remaining cases, where second-order filters are used, it can be seen that spurious side force cues will be reduced as the sway-axis break frequency, ω_{hpy}, reduces (i.e. increasing coordination). However, as the sway-axis break-frequency reduces the amount of simulator displacement increases, placing a practical limit on the lower value of ω_{hpy}. Figure 13b shows the specific force produced using third-order sway-axis filters with varying roll-axis filter break frequency, $\omega_{hp\phi}$. It can be seen that as $\omega_{hp\phi}$ reduces the spurious side force cues increase. If the simulator is rolling to a larger angle and remaining displaced for longer, as is the case for small values of $\omega_{hp\phi}$ (Fig. 12a), then intuitively we can see that the amplitude of the side-force due to tilt cue must be larger. Analytically, it can also be shown that as

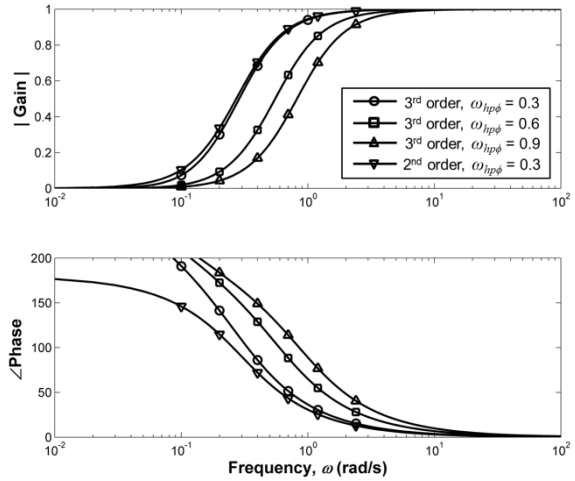

Figure 14. Classical washout roll-axis frequency response

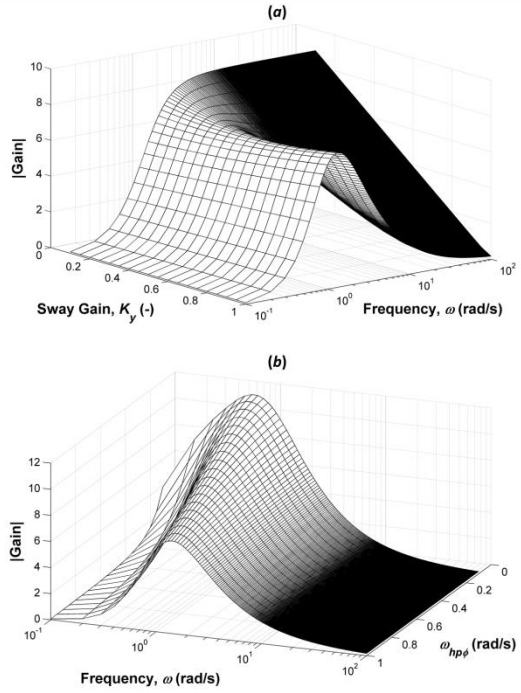

Figure 15. Classical washout specific force error amplitude

$\omega_{hp\phi}$ increases then the frequency dependent gain of the roll-axis filter, $K_\phi HP_\phi$, will decrease over the low frequency range (Fig. 14) which is as another way to reduce the specific force error (see previous discussion and Equation (8)).

The roll-axis input to output transfer function is given by Equation (14).

$$\frac{\phi_c}{\phi}(s) = K_\phi HP_\phi \qquad \ldots(14)$$

Figure 14 shows the frequency response of the roll channel, the gain and phase relationships between the input and output variables, in the form of a Bode plot. It can be seen from Fig. 14 that as $\omega_{hp\phi}$ increases, so too does the frequency dependent phase lead between the aircraft model roll attitude (input) and the motion platform roll command (output). The advantage of the second-order filter is the reduced phase lead at low frequencies.

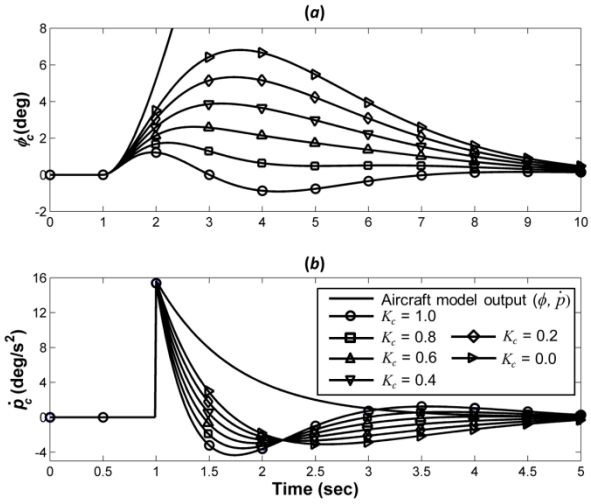

Figure 16. Lm^2 roll response

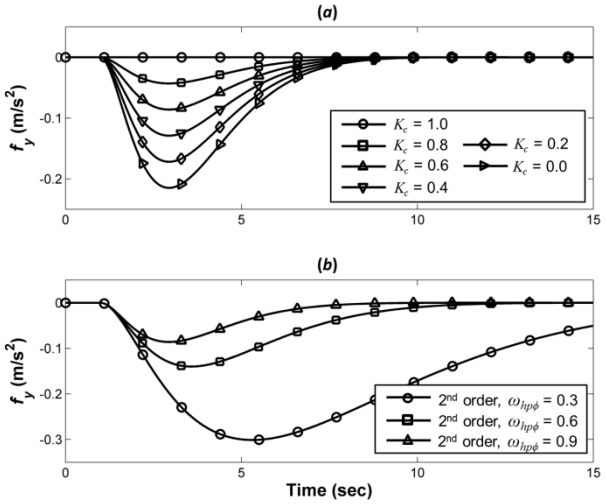

Figure 17. Lm^2 lateral specific force

The specific force error to roll input transfer function is approximately (ignoring the transient roll acceleration term) given by Equation (15).

$$\frac{f_y}{\phi}(s) = gK_\phi HP_\phi\left(K_y HP_y - 1\right) \qquad \ldots(15)$$

The amplitude of this transfer function is presented in Fig. 15. Fig. 15a shows the shape of the amplitude with varying values of the sway gain, K_y. At high values of K_y the amplitude response resembles a smooth peak with the position and amplitude of the peak being largely determined by the sway-axis filter break frequency, ω_{hpy}. However, at low values of K_y the response begins to approximate the 'S'-shaped characteristic of the roll-axis amplitude function shown in Fig. 14. Finally, Fig. 15b shows how the amplitude of the specific force error changes with roll-axis break frequency, $\omega_{hp\phi}$, for a fixed sway gain, K_y.

In summary it can be seen that the roll response of the classical washout algorithm is influenced by the roll-axis motion filter gain, K_ϕ, and break frequency, $\omega_{hp\phi}$. A low

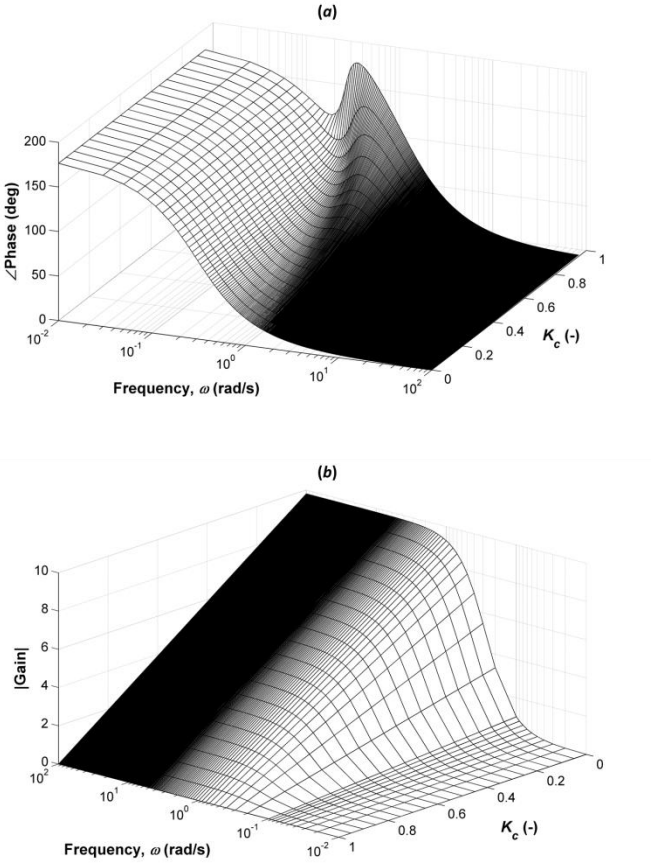

Figure 18. Lm^2 (a) Roll transfer function phase, (b) Specific force error amplitude, with a second-order sway-axis filter

break frequency is desired to reduce the washout strength (Fig. 12) and phase distortion (Fig. 14). The sway response of the classical washout algorithm is influenced not only by the sway-axis motion filter gain, K_y, and break frequency, ω_{hpy}, but also by K_ϕ and $\omega_{hp\phi}$. Increasing $\omega_{hp\phi}$ will reduce the severity of the specific force false cues by reducing the amplitude and duration of the simulator's roll response (Figs. 13 and 15). Alternatively, reducing ω_{hpy} (Fig. 13) or increasing K_y will also reduce the severity of the false cues by increasing the lateral coordination (and hence simulator lateral displacement). From Equation (8) it can also be seen that reducing K_ϕ will reduce the severity of the lateral false cue by reducing the peak simulator roll angle.

Lateral Manoeuvring Motion:

Figure 16 shows the roll acceleration and displacement response of the Lm^2 algorithm with varying values of coordination gain, K_c (K_ϕ = 1 and $\omega_{hp\phi}$ = 0.6). It can be seen that varying K_c will vary the shape and amplitude of the platform roll displacement. When K_c is unity the roll output is proportional to the lateral acceleration, $\ddot{y}_{roll}/g$, because the full amount of ϕ_{hp} is passed through the feedback network (Fig. 9), cancelling the output from the roll-axis filter. Intermediate values of K_c lead to less distortion and, when K_c is zero, the roll output is equal to ϕ_{hp}, since the feedback network is effectively removed (i.e. no feedback from ϕ_{hp} or $\ddot{y}_{roll}/g$). The coefficients of the roll-axis motion filter also

influence the shape of the roll response. The roll-axis break frequency, $\omega_{hp\phi}$, will have a similar effect to that discussed in the classical washout example, in that it will change the amplitude and duration of the simulator's roll displacement and the gain, K_ϕ, will scale the amplitude.

The lateral specific force experienced by the pilot is shown in Fig. 17. The relationship between the lateral specific force and the filter coefficients is simplified in the Lm^2 algorithm when compared to the classical washout algorithm. For Lm^2 the specific force response is influenced only by K_ϕ and $\omega_{hp\phi}$ (Fig. 17b), and by the coordination gain, K_c (Fig. 17a). The choice of sway-axis filter order or break frequency has no bearing on the shape of the response (see Equation (12)). It can be seen from Fig. 17a that the peak in specific force error reduces as K_c is increases. In common with the classical washout algorithm, when $\omega_{hp\phi}$ is reduced then intuitively we see that both the amplitude and duration of the specific force error will increase (Fig. 17b). However, when K_c is unity then full coordination (zero specific force error) is always achieved, regardless of the value of any other coefficient.

The roll-axis input to output transfer function is given by Equation (16).

$$\frac{\phi_c}{\phi}(s) = K_\phi HP_\phi\left(1 - K_c + K_c HP_y\right) \qquad \ldots(16)$$

It can be seen from Equation (16) that if K_c is zero, then the transfer function will be identical to the classical washout roll-axis filter (Equation (14)). However, if K_c is unity then the output is a function of both the roll and sway-axis motion filters. Figure 18a shows the phase lead between the aircraft model roll attitude (input) and the motion platform roll command (output). Using a second-order sway-axis filter, HP_y, makes the total roll-axis transfer function 4th order; an undesirable side-effect of this is the large peak in phase distortion with high values of K_c, centred on the sway-filter break-frequency. At low values of K_c the phase lead more closely resembles the smooth 'S-shape' characteristic of the classical washout algorithm (Fig. 14).

The specific force error to roll input transfer function is given by Equation (17).

$$\frac{f_y}{\phi}(s) = gK_\phi HP_\phi(K_c - 1) \qquad \ldots(17)$$

This is simplified compared to the equivalent classical washout transfer function (Equation (15)) and shows that only the roll-axis motion filter and the coordination gain have any influence on the specific force error. It is also clear that, as previously discussed, when K_c is unity then full coordination is achieved and the resulting specific force error is zero. Figure 18b shows the amplitude of this transfer function with varying values of K_c.

In summary it can be seen that the roll response of the Lm^2 algorithm is influenced by the roll-axis motion filter gain, K_ϕ, and break-frequency, $\omega_{hp\phi}$, and significantly by the coordination gain, K_c (and to an extent the sway-axis filter break frequency, ω_{hpy}). Varying the roll-axis filter coefficients has the same effect as with the classical washout algorithm. However, large values of K_c introduces distortion to the roll response, by increasingly weighting the roll output, ϕ_c, away from the roll-axis filter output, ϕ_{hp}, and towards the sway-axis filter output, $\ddot{y}_{roll}/g$. In contrast the same feedback arrangement simplifies the relationship between the roll angle input and specific force error. Full coordination can be achieved when the coordination gain, K_c, is unity. Reducing K_c decreases the lateral coordination and, therefore, leads to an increase in spurious side force cues when compared to the fully coordinated case.

Experimental Setup

Simulator Facility

The HELIFLIGHT-R simulator facility at the University of Liverpool is a fully re-configurable research simulator[21], consisting of a generic rotorcraft cockpit housed inside a 12ft diameter visual display dome, mounted on a short stroke (24in) electric motion platform (Fig. 19). The motion platform is capable of roll-axis displacements of ±23º and sway-axis displacements of ±0.46m. However, these are maximum displacement capabilities, for motion in a single axis; simultaneous motion in multiple axes will severely restrict the available motion envelope. The outside world image has a field-of-view of 210º (±105º) by 70º (+30º/-40º).

Figure 19. Heliflight-R flight simulator

Task

The course layout for the roll-sway sidestep task is shown in Fig 20. The task was performed in a detailed airfield environment in front of a model of the NASA Ames hover-boards[22]. Starting with the aircraft aligned with the left-hand target-board, the pilot must perform a 40ft lateral sidestep, to reposition the aircraft at the opposite target. Desired performance was achieved when the opposite target was captured within six seconds, with a single overshoot or undershoot around the target position of less than ±3.5ft.

Adequate performance was achieved when the pilot captured the opposite target within 10 seconds, with a single overshoot or undershoot of ±6ft. The pilot was able to judge capture performance by observing the relative position of the red ('V'-shaped) target markers against the yellow and black background boards. The task was conducted in good visibility with no atmospheric turbulence.

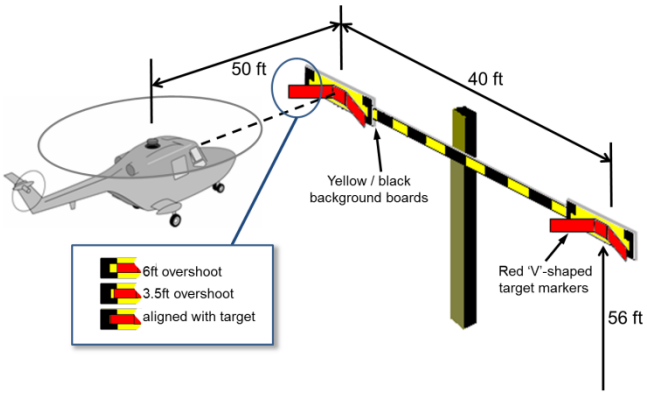

Figure 20. Roll-sway sidestep task course layout

Vehicle Dynamics

The pilot controlled lateral position of the vehicle through roll attitude using lateral cyclic stick inputs. Roll-sway vehicle dynamics are given by Equations (1) and (2) and are representative of a hovering helicopter with a roll-rate command system and height-hold auto-pilot. The normalised roll damping derivative, L_p, was set to -4.5 sec^{-1} and the lateral cyclic sensitivity, L_δ, was selected to give a roll acceleration of ±2 rad/s^2 for full lateral cyclic deflections; these values are typical of a moderately agile helicopter.

Motion Configurations

Classical Washout:

The classical washout algorithm filter coefficients examined in this experiment were taken from Ref. 15 and are shown in Tables 1 and 2. Both the roll and sway-axis motion filters were third-order (see Equation (5)) with damping ratios, $\zeta_{hp\phi}$ and ζ_{hpy}, set to 0.9 and first-order break-frequencies, $\omega_{b\phi}$ and ω_{by}, set equal to 0.1 rad/s. Three additional roll-axis filters were tested in addition to those investigated in Ref. 15 to give an intermediate roll-axis break frequency of 0.6 rad/s (Configurations A8, A9 and A10).

Lateral Manoeuvring Motion:

The number of Lm^2 configurations tested was limited due to time constraints. Based on the results of the parametric study (described in the previous section) it was decided to concentrate effort on examining the effects of varying the coordination gain, K_c. The sway-axis filter was implemented as a second-order filter to restrain the platform's lateral motion within the available envelope. The tested configurations are shown in Table 3. In each case the damping ratios, $\zeta_{hp\phi}$ and ζ_{hpy}, were set to 0.9.

Config	K_ϕ	$\omega_{hp\phi}$ (rad/s)	at 1 rad/s Gain (-)	at 1 rad/s Phase (deg)
A1	0.11	0.3	0.1	36
A2	0.21	0.3	0.2	36
A3	0.32	0.3	0.3	36
A4	0.17	0.9	0.1	89
A5	0.33	0.9	0.2	89
A6	0.42	0.9	0.3	89
A7	Fixed Base – No Motion			
A8	0.12	0.6	0.1	65
A9	0.25	0.6	0.2	65
A10	0.38	0.6	0.3	65

Table 1. Roll motion filter configurations

Config	K_y	ω_{hpy} (rad/s)	at 1 rad/s Gain (-)	at 1 rad/s Phase (deg)
T1	0.16	0.9	0.1	89
T2	0.33	0.9	0.2	89
T3	0.5	0.9	0.3	89
T4	0.66	0.9	0.4	89
T5	Fixed Base – No Motion			

Table 2. Sway motion filter configurations

Config	K_c	K_ϕ	$\omega_{hp\phi}$ (rad/s)	ω_{hpy} (rad/s)
L1	0.1	0.2	0.3	1.4
L2	0.3	0.2	0.3	1.4
L3	0.4	0.2	0.3	1.4
L4	0.5	0.2	0.3	1.4
L5	0.6	0.2	0.3	1.4
L6	0.7	0.2	0.3	1.4
L7	0.2	0.3	0.3	1.4
L8	0.3	0.3	0.3	1.4
L9	0.4	0.3	0.3	1.4
L10	0.5	0.3	0.3	1.4

Table 3. Lm^2 filter configurations

Experimental Procedures and Measures

Two pilots took part in these experiments both were qualified military rotary-wing test pilots. The first pilot (Pilot A) assessed the classical washout algorithm and the results of this experiment are reported here and in Ref. 15. The second pilot (Pilot B) assessed both the classical washout (including the additional configurations A8-A10) and Lm^2 algorithm, and those results are reported in this paper. Both pilots were briefed that they would experience a range of motion cues, but were given no specific details regarding the nature of the cues or the motion filter configurations. The pilots were presented with each configuration in a random order and given as many opportunities as necessary to repeat the task, but must perform the task at least five times before providing a rating. Subjective ratings were taken from the Motion Fidelity Rating Scale (Fig. 21). Further details regarding the development of this rating scale are given in Ref. 23.

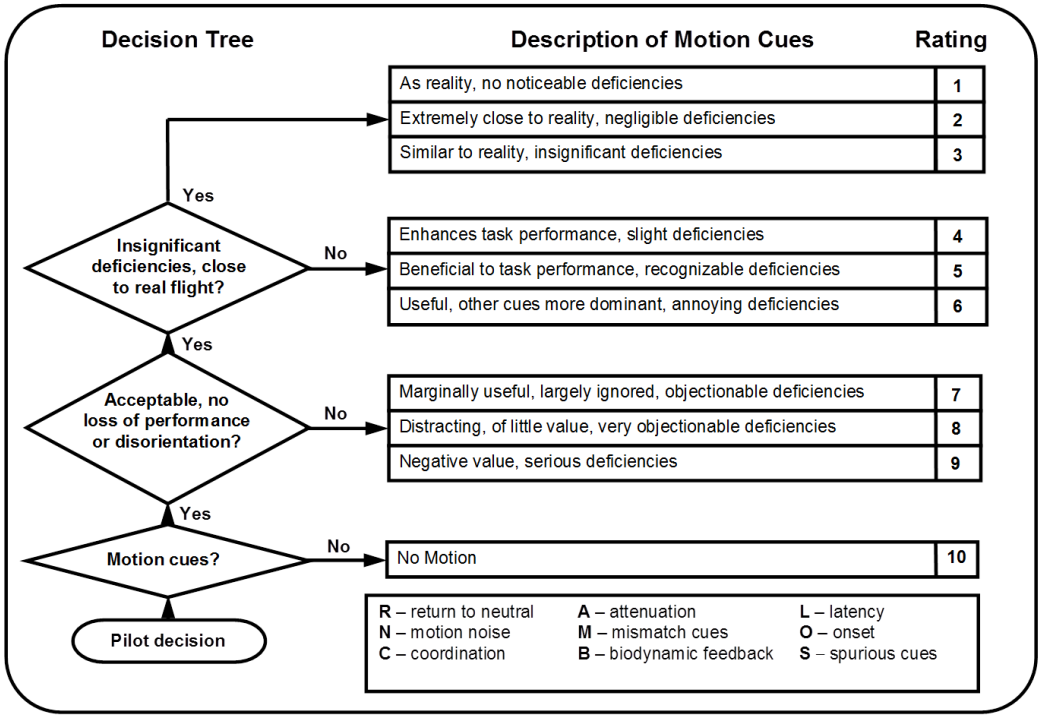

Figure 21. Motion Fidelity Rating Scale

Results

The results of the experiment will now be discussed in terms of five key relationships: (i) the effects of introducing motion cues compared to the no-motion case; (ii) the effects of increasing the sway motion gain on the classical washout algorithm; (iii) the effects of increasing the roll motion gain and break frequency on the classical washout algorithm; (iv) the effects of increasing the coordination gain on the Lm^2 algorithm and, finally, (v) a comparison of the classical washout and Lm^2 algorithms.

Motion versus no-motion

Figure 22 shows one pilot's cyclic activity and the phase-plane portrait for a number of sidestep manoeuvres, performed with and without motion cues. Phase-plane portraits provide a concise means of describing a trajectory, by plotting the time history of a given variable on the horizontal axis against its derivative on the vertical axis. In Fig. 22 lateral position is plotted on the horizontal axis and lateral velocity is plotted on the vertical axis. It can be seen that without motion cues the pilot could not consistently achieve the desired performance criteria and was over-controlling, i.e. applying large oscillatory inputs. Positioning accuracy was poor without motion cues and several large overshoots and undershoots are evident around the target locations (±20ft). On the other hand, with appropriately tuned motion cues, positioning accuracy was good with only a few small overshoots and undershoots around the targets. Without platform motion, the vehicle acceleration cues, which normally aid the pilot to anticipate (or lead) during position capture and stabilisation are absent. The pilot must, therefore, compensate by adjusting his control strategy based on the remaining (mainly visual) cues. As Pilot B explained – '[During stabilisation] *just before the aircraft starts moving* [visually] *the* [motion] *cues give you the predictability of when to take bank angle off. Whereas purely on visuals you're already moving in the other direction before you can take the bank angle off*'. In the event the pilot was not able to accomplish the task successfully without motion cues. It is conceivable that, given practice, desired performance could be achieved without motion cues, but the training implications of pilots adapting their control strategy compared to real flight are potentially very serious.

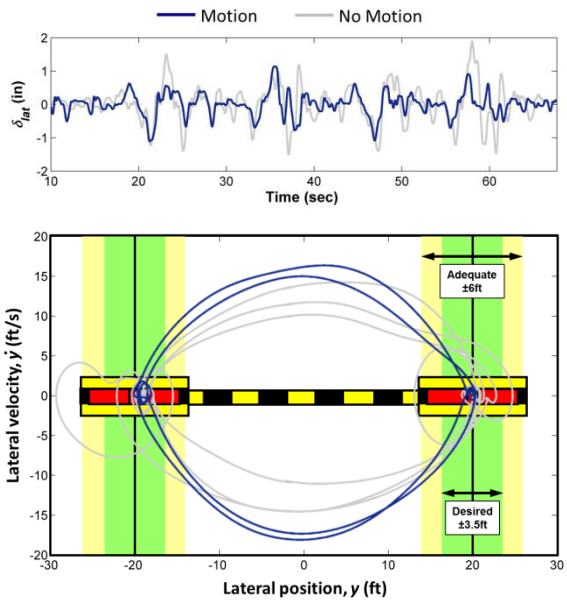

Figure 22. Lateral stick activity (top) and phase plane portrait (bottom) with motion and no motion

Classical Washout: Increasing Sway Gain

Figure 23 shows the motion fidelity ratings with increasing sway-axis motion gain, K_y, for the classical washout algorithm. The ratings are given for both pilots with the symbols representing the average rating and bars showing the minimum and maximum ratings (in cases where there are no min/max bars then the two pilot ratings are identical). In general the agreement between the pilot's ratings is very encouraging, usually being within a single point of each other. There are only two situations where this is not the case, and these occurred at the lowest and highest sway motion gains.

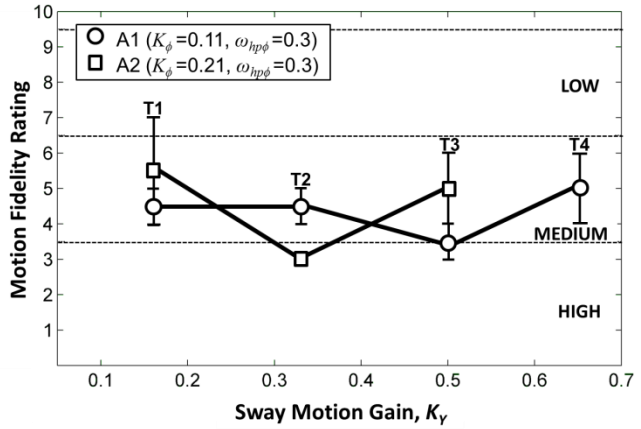

Figure 23. Motion fidelity ratings with increasing sway gain

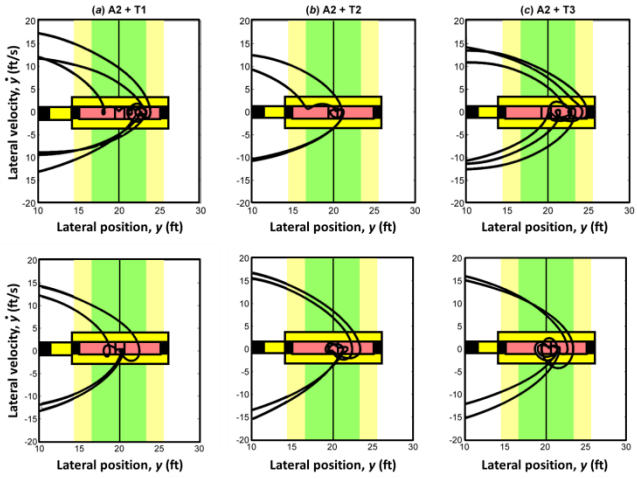

Figure 24. Phase plane portraits with increasing sway motion gain (top row Pilot A, bottom row Pilot B)

At low values of sway gain (coupled with the higher roll gain – Config A2+T1), Pilot A described the motion cues as '*abrupt*' and '*harsh*', because of accelerations induced at the pilot's seat by platform roll motion, returning an rating of 7. Pilot B described the roll motion cues in a very similar way, saying - '*You get a big sharp kick when you roll*' and adding that in the real aircraft the roll motion cues would probably be less '*peaky*'. However, Pilot B found the sharper motion cues less objectionable, noting that they aided him in stopping and stabilising at the target position, and as a result gave a rating of 4. This disparity in subjective ratings might simply reflect differences in personnel preference between the two pilots, or may be related to the type of aircraft, and hence anticipated roll response to stick input with which each pilot is most familiar.

As the sway gain increased both pilots' perceptions of the motion cues improved. Apart from at the highest sway gains, where both pilots had issues with the motion cues. Pilot A gave a rating of 6 at the highest sway motion gain with the higher roll motion gain (A2+T3), citing motion noise and washout sensation as the primary causes. Pilot B gave a rating of 6 at the highest sway motion gain with the lower roll gain (A1+T4) also citing motion noise, along with a lack of coordination between the visual and motion cues, adding that – '*At initial stick application the amount of motion was giving the impression that you were about to move sideways a lot faster than perceived through the visual cues*' this affected his perception of the closure rate and made stabilisation at the target position very difficult. Figure 24 shows examples of the phase plane portraits with increasing sway motion gain (left to right), for the right-hand target capture portion of the manoeuvre only. It can be seen from Fig. 24 that pilot performance is well correlated with the subjective ratings.

Classical Washout: Increasing Roll Gain and Break-Frequency

Figure 25 shows the pilots' motion fidelity ratings with three different roll-axis motion filter break-frequencies. The ratings for break-frequencies of 0.3 and 0.9 rad/s are given for both pilots A and B. Again the symbols represent the average rating. The break frequency of 0.6 rad/s was only assessed by Pilot B. Nevertheless, where ratings for both pilots are available then they are in excellent agreement.

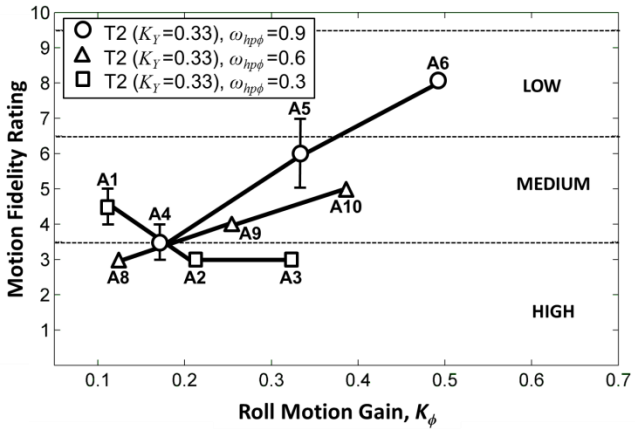

Figure 25. Motion fidelity ratings with increasing roll gain

At the lowest break-frequency, $\omega_{hp\phi}$ = 0.3 rad/s, pilot opinion either improves or remains constant with increasing roll motion gain. However, both pilots disliked configurations with higher break-frequencies. At the highest break frequency, $\omega_{hp\phi}$ = 0.9 rad/s, and highest roll motion gain (A6), both pilots objected strongly to the motion response, describing the motion cues as '*ratchety*' and '*sharp*', and identified biodynamic feedback as a factor in their ratings. At the reduced roll motion gain (A5) both commented on poor coordination between the motion and

visual cues. Pilot B was obviously more affected by this cue mismatch than Pilot A, commenting on a feeling of '*disorientation*', hence awarding a rating of 7. The results for the intermediate break frequency, $\omega_{hp\phi}$ = 0.6, follow a very similar trend.

The pilots' comments reflect the stronger washout (i.e. greater attenuation of low frequency, sustained roll motion cues) and the increased phase shift between the vestibular and the visual motion cues, resulting from the increase in break frequency (see Figs. 12 and 14). The effect of increasing the roll motion filter break-frequency on the platform roll response is illustrated in Fig. 26, which shows the motion platform roll rate for a single sidestep manoeuvre. The solid grey line is the platform roll rate command by the motion drive algorithm, $\dot{\phi}_c$, the dotted grey outline is the achieved platform roll rate measured by a sensor mounted inside the cockpit, and the solid black line is the roll rate that would be commanded if the roll-axis motion filter, HP_ϕ, was removed from the classical washout algorithm, thus removing the source of the phase shift (i.e. if HP_ϕ = 1 in Fig. 8 then the commanded roll rate would be equal to the outside world visual roll rate, $\dot{\phi}$, scaled by the roll motion gain, K_ϕ). It can be seen that at the lowest break-frequency, the platform roll rate and the visuals roll rate are in very close agreement. However, at the higher break-frequency, significant distortions are introduced by the washout filter. These distortions will, of course, manifest themselves as a mismatch between vestibular motion cues and the cues from the visual scene.

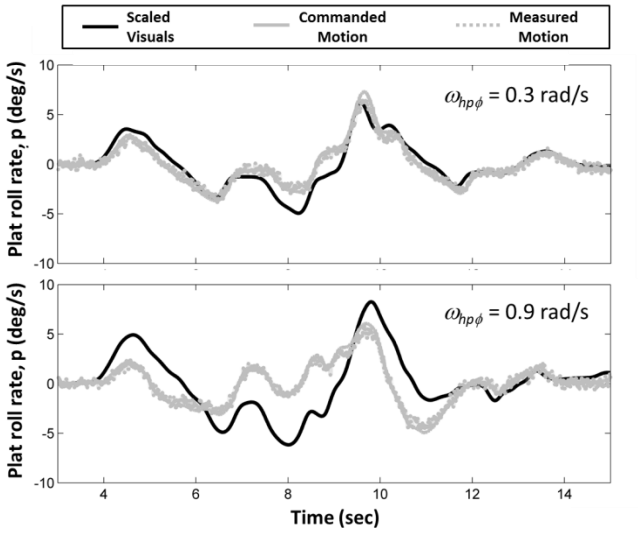

Figure 26. Motion platform roll rate with two different motion filter break-frequencies

The subjective ratings shown in Fig. 25 are striking, both in terms of the trends and the agreement between the two pilot subjects. They tell us that for break-frequencies of 0.6 and 0.9 rad/s, then the only way to improve pilot opinion is to reduce the roll motion gain, effectively masking the problem by reducing the amplitude of the roll motion cues, and making the vestibular motion to visual motion cue mismatch less obvious.

Lm^2: Increasing Coordination Gain

Figure 27 shows the pilot's motion fidelity ratings for the Lm^2 algorithm with increasing coordination gain, K_c, at two different roll motion gains. Only Pilot B assessed the Lm^2 algorithm, so the ratings in Fig. 27 are representative of only a single pilot opinion. However, where possible each run was repeated several times in order to ensure a consistent rating. The open symbols in Fig. 27 represents an average rating taken from a number of runs, closed symbols are used where data is only available for a single run. It can be seen that the ratings awarded by Pilot B were generally very repeatable and normally within a single point of each other.

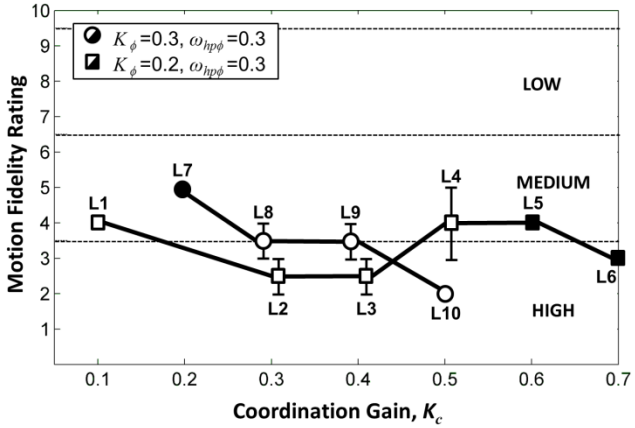

Figure 27. Motion fidelity ratings with Lm^2 algorithm at varying coordination gain

The most favourable, and consistent, ratings were given for a coordination gain of 0.5 at the higher roll motion gain (L10). With this configuration the pilot felt that the motion cues were predictable, allowing him to be aggressive during corrections at the target position. Interestingly, the pilot suggested that, with those motion cues, the visuals were now letting the simulation down and felt that he could have performed the task even better with a higher resolution visual display. The only criticism was that the motion cues might have been '*slightly above reality*'. It is possible that had a coordination gain of greater than 0.5 been tested, then the pilot may have preferred that configuration. However, with the limited motion envelope available it was not possible to test higher coordination gains without risking saturation of the actuator legs.

When the coordination gain was reduced to 0.4 (L9) and 0.3 (L8) then the pilot's subjective ratings degraded. The pilot commented that the motion cues were still very good with these configurations, especially for large stick inputs, but for smaller stick inputs the platform motion didn't follow the visuals as closely, in his words – '*The motion cues to the initial input were reasonably well coordinated, but something made stabilisation not as crisp*'. The pilot's perception therefore, depended on how aggressively he attacked the manoeuvre and the number of small corrections which were required to stabilise at the target position. This is reflected in the subjective ratings for configurations L8 and L9 which lie on the high/medium fidelity border. At a

low coordination gain of 0.2 (L7) there is a clear degradation in the motion cues. The pilot complained that he had to keep the aggression level low in order to successfully complete the task with that configuration, adding – '*when roll angles (cyclic inputs) are low then the motion cues are good, but for moderate angles of bank there is a mismatch between the motion and visual cues*'.

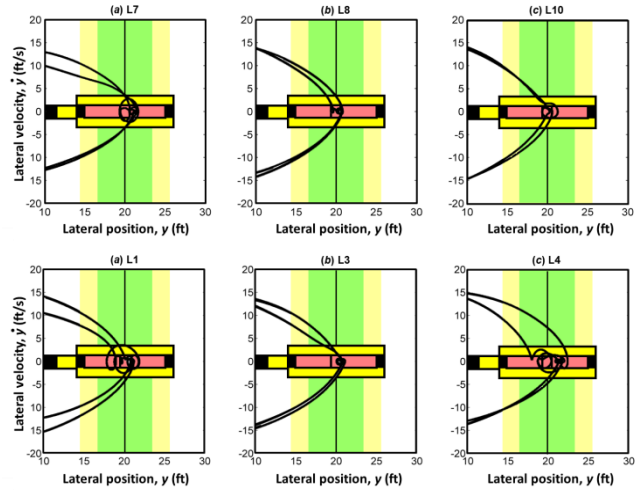

Figure 28. Phase plane portraits with increasing coordination gain (top row K_ϕ=0.3, bottom row K_ϕ=0.2)

The top row of Fig. 28 shows the phase-plane portraits of three target captures at the right-hand board, with increasing coordination gain at a roll motion gain, K_ϕ, of 0.3. Although desired performance was achieved in each case, there are still some interesting differences. Firstly, it can be seen that the pilot's ability to stop and stabilise at the target position, with accuracy, is significantly improved at the higher coordination gains. Secondly, at the higher coordination gains the pilot was performing the sidestep task more aggressively, as evident from the higher lateral velocity used to approach the target board. Note that although the capture performance for a K_c of 0.5 (L10) in Fig. 28 looks worse than for a K_c of 0.3 (L8), the number of corrections needed to acquire the target position are actually fewer and are accomplished using larger (more aggressive) pilot inputs (see Fig. 29).

The bottom row of Fig. 28 shows the phase-plane portraits of three target captures at the right-hand board, with increasing coordination gain at a roll motion gain, K_ϕ, of 0.2. Again desired performance was achieved in each case. However, this time there are more significant differences between the three plots. The best performance was clearly obtained with a K_c of 0.4 (L3) and degrades at the lower and higher values of coordination gain. This correlates well with the pilot's subjective ratings.

Figure 29 compares the time histories of a single sidestep manoeuvre (left to right) for two different values of coordination gain. At the higher coordination gain, K_c = 0.5 (L10), it can be seen that the pilot is much more positive when applying stick inputs at the start and end of the manoeuvre. With the higher coordination gain the pilot applies a positive input to start the manoeuvre, reverses the input to roll 'wings' level approximately half way through the sidestep and then puts on opposite bank to stop at the target position. Finally, at the end of the manoeuvre the pilot makes a small number of positive corrections to stabilise at the target location with little or no overshoots or undershoots. On the other hand, at the lower coordination gain, K_c = 0.2 (L7), the pilot's inputs at the start and end of the manoeuvre are not nearly so positive and large oscillatory cyclic inputs are evident during stabilisation at the target location. This analysis compares well with the pilot's comments and reflects a general lack of confidence in the motion cues at very low values of coordination gain.

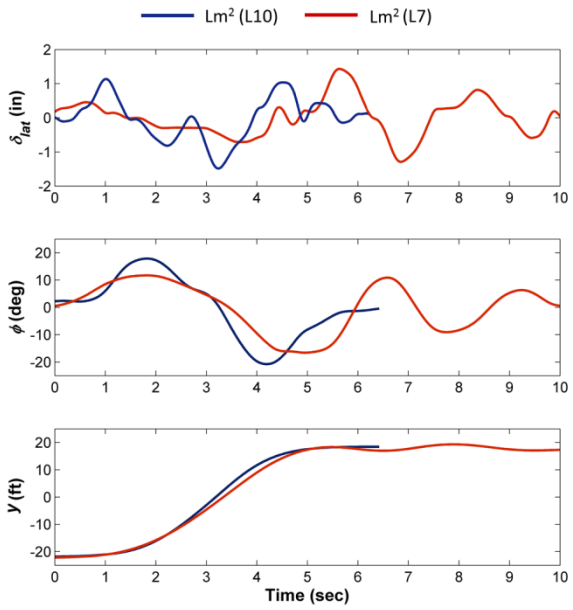

Figure 29. Time history of target capture at two different coordination gains

Figure 27 shows the pilot's subjective ratings for increasing coordination gain at a lower roll motion gain (L1-L6). These results follow the same trend for coordination gains below 0.5 as they did for the higher roll motion gain. However, for coordination gains of above 0.5 the subjective ratings start to degrade again. At first this may seem a surprising result, as one might expect the ratings to continue to improve as the coordination gain is increased. One possible explaination can be found in the pilot's comments for these runs, where the relative contribution of roll and sway motion cues is discussed – '*Initial bank angle gives good positive cueing, after that it felt like the sim was just moving laterally. You wouldn't get that much sideways motion. The blend between roll and sway is all wrong.*'. Clearly, harmonisation between motion in the roll and sway axes is as important for the Lm^2 algorithm as it is for the classical washout algorithm. At a low roll motion gain it is possible that the higher coordination gains lead to sway axis motions which appear to overpower the roll motion. This is similar to the results obtained for the classical washout algorithm (see Classical Washout: Increasing Sway Gain). Further testing of the Lm^2 algorithm focussed on changes to the roll and sway-axis filter break-frequencies. The results

of these tests are not reported here, as they were in no way as clear and compelling as similar results for the classical washout filter (see for example, the results of the classical washout algorithm with increasing roll break-frequency, Fig. 25). It is difficult to explain why this should be the case, although the input to output relationship, particularly in the roll-axis, is clearly less direct for the Lm^2 algorithm due to the additional feedback loop (see earlier parameteric study). It does, however, suggest that the process of motion tuning may, possibly, be more challenging for the Lm^2 algorithm than for the classical washout with its more direct input to output relationship.

Classical Washout Compared to Lm^2

The pilot who assessed both the classical washout and Lm^2 algorithms (Pilot B) clearly preferred the motion response of the Lm^2 algorithm, describing the motion cues as '*predictable*'. Lm^2 allowed the pilot to use more aggressive cyclic inputs to make small accurate corrections during stabilisation at the target position, while still giving good initial onset cues. The pilot generally felt that the Lm^2 motion response – '*felt more like a real airplane*' and conversly commented that with the classical washout – '[it was] *obvious that you are in a simulator*'. Figure 30 compares the time histories of the motion platform response during a single sidestep manouvre (left to right) with Lm^2, K_c = 0.5 (L10), and two classical washout configurations (A2+T2 and A2+T3). It can be seen from Fig. 30 that althought the roll response of the platform is broadly similar, the lateral specific force is reduced for Lm^2.

The difference in the way that the motion platform moves with the Lm^2 algorithm, compared to the classical washout, is striking when observed from outside the simulator cabin. Figure 31 shows the roll and lateral motion of the platform for the Lm^2 algorithm and Fig. 32 shows the same for the classical washout. The pictorial representations of the simulator above each plot shows the approximate pose of the platform at each instant in time, as viewed from the front of the simulator (i.e. opposite to the pilot). Clearly, the motion platform was more active with the Lm^2 algorithm and it would tilt and translate simultaneously, unlike the classical washout algorithm. The additional platform activity with Lm^2 was noted by the pilot, prompting the comment – '*Lots of noise, lots and lots of noise*' referring to the mechanical noise generated by the platforms mechanisms. However, this did not appear to have a negative effect on the pilot's opinion of the Lm^2 algorithm. Figures 33 and 34 show the amount of motion platform envelope used by the Lm^2 (Fig. 33) and classical washout algorithms (Fig. 34). These plots demonstrate clearly the differences in the way the motion platform moves for each of the algorithms.

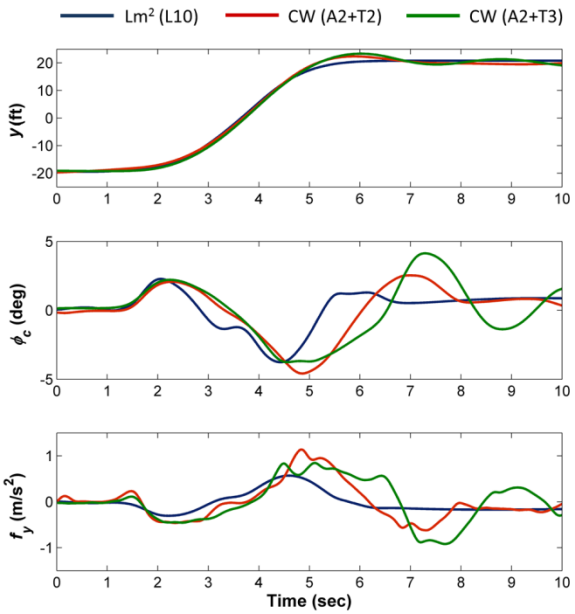

Figure 30. Time history of target capture with Lm^2 and two classical washout configurations

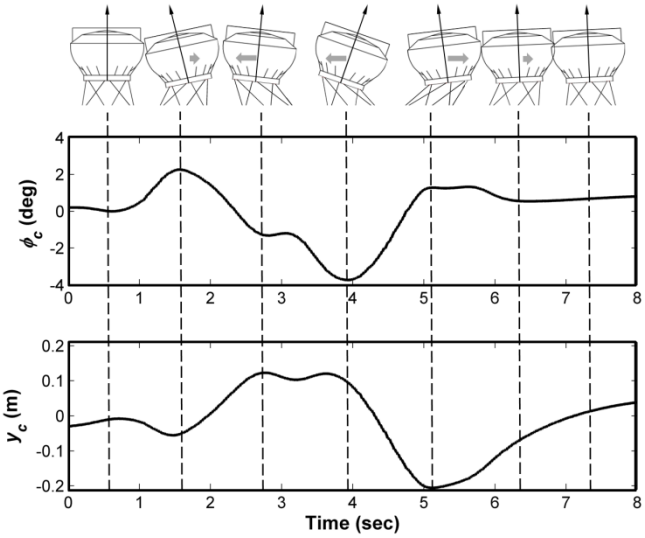

Figure 31. Platform roll and lateral motion Lm^2 algorithm

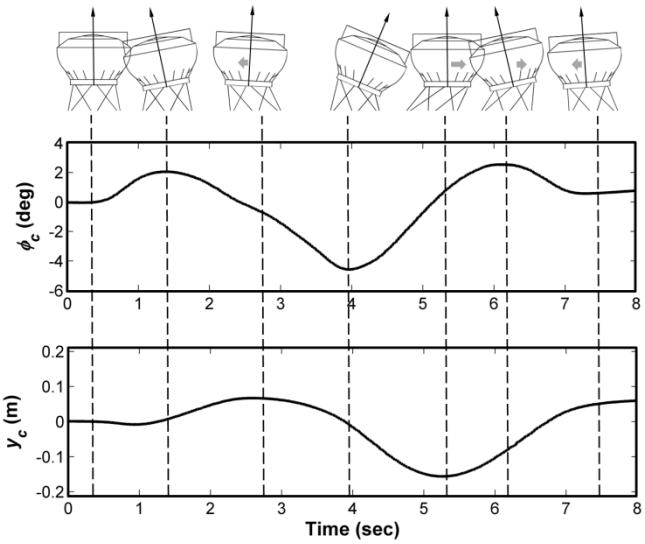

Figure 32. Platform roll and lateral motion classical washout algorithm

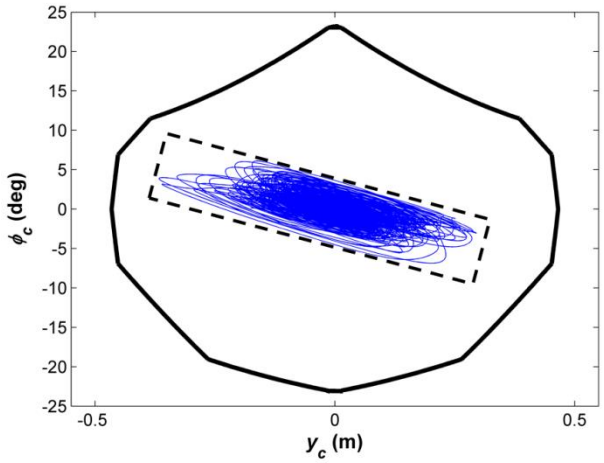

Figure 33. Usable motion platform envelope with Lm^2 motion trajectories

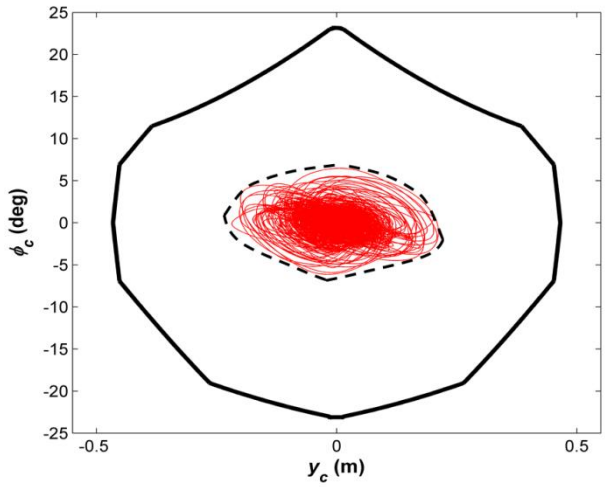

Figure 34. Usable motion platform envelope with classical washout motion trajectories

Discussion

The first objective of this experiment was to repeat the previous roll-sway experiment reported in Ref. 15. The current experiment was conducted on the same simulator facility with the same aircraft model, task and motion drive algorithm as the previous experiment. The aim of the current work was to determine if the results gathered from this previous experiment were repeatable for a different subject pilot. The subjective ratings presented in Figs. 23 and 25 show that, where ratings for both pilots are available, they are in very good agreement, often being within one rating of each other. Reference 24 describes this as low 'interpilot' variability. This is an encouraging result which demonstrates that the Motion Fidelity Rating scale is being used and interpreted consistently by pilots. The consistent and repeatable application of pilot ratings is clearly an important factor in the success of any subject rating scale. In a small number of cases disparities between ratings were observed e.g. at the lowest sway gain with the highest roll gain (Fig. 23), where Pilot A gave a rating of 7 corresponding to low fidelity, and Pilot B returned a rating of 4 corresponding to medium fidelity. Notably, in all of these cases both pilots described the motion cues in a very similar way. It is possible that these disparities simply reflect differences in the personnel preferences, training and background of each pilot, for example, the type of aircraft which each pilot is most familiar with. Even when pilots have similar training, experience on a similar aircraft and comparable amounts of flight time, they will not necessarily have the same performance or use the same piloting strategy to accomplish a specific task. These differences make some 'interpilot' variability inevitable in any experiment.

An important result from the previous experiment (Ref. 15) was the dominant effect which roll-axis break frequency had on perceived motion fidelity. In Ref. 15 two roll-axis break-frequencies where tested, 0.3 and 0.9 rad/s. Reference 15 reports that with the highest break frequency, leading to mismatch (phase shift) between the visual and vestibular cues, the only way to improve perceived fidelity was to reduce the roll motion gain. Whereas, at the lowest break frequency pilot opinion either improved or remained constant with increasing roll motion gain. In the current experiment the same two break-frequencies were tested, along with an intermediate break frequency of 0.6 rad/s. The intention was to determine if there was a threshold between the two previously tested break-frequencies, where pilots were indifferent to this cue mismatch. The agreement between the two pilots was excellent for the two previously tested break-frequencies (Fig. 25). In addition, the results for the intermediate break-frequency show that, even at 0.6 rad/s, there is still too much phase shift introduced between the vestibular and visual cues. Although the vestibular-visual cue mismatch was clearly less objectionable at 0.6 rad/s than it was at 0.9 rad/s. In Ref. 7 Bray found that a roll-axis break frequency of 0.5 rad/s led to pilot complaints of slight contradictions between visual and motion cues, which is a very similar finding, particularly when compared to the intermediate break frequency examined in this experiment. Finally, in Ref. 2, Sinacori gives the following advice for anyone involved in tuning motion systems – '*Increase the washout* [break] *frequencies slowly and listen for pilot comments regarding disorientation and nausea. Listen to him, and try to relate his comments to the monitor data. They will agree remarkably well*', the results of this and the previous experiment would clearly support Sinacori's advice.

The second objective of this experiment was to examine the Lm^2 algorithm, which is a modification to the classical washout algorithm used in the previous experiment. The pilot who assessed the Lm^2 algorithm described the motion cues as '*predictable*' and remarked that it allowed him to use more aggressive (i.e. larger) cyclic inputs when making small corrections during stabilisation at the target position. The pilot generally felt that the Lm^2 motion response – '*felt more like a real aircraft*', on the other hand he felt that with the classical washout - '[it was] *obvious that you are in a simulator*'. Similar comments have been made by other pilots during evaluations of the Lm^2 algorithm in fixed-wing training simulators (Ref. 19), although these were not

gathered as part of a systematic experiment. The pilot in our experiment had no prior knowledge of, or exposure to the Lm^2 algorithm and was not told which algorithm he was evaluating during each run. The exact source of the apparent enhancement in cueing fidelity provided by Lm^2 is not clear, but there are three main areas where the implementation of the Lm^2 and classical washout algorithms differ :–

(i) The feedback mechanism added to the output of the Lm^2 roll channel (see Fig. 9) to coordinate the roll and lateral cues.
(ii) The Lm^2 algorithm inputs are specific force and rotational rates at the pilot position, rather than at the platform's motion centroid.
(iii) In this experiment at least, the Lm^2 algorithm used second-order motion filters rather than third-order.

Of these differences the first two are likely to be most significant and the second and third could easily be added to the classical washout algorithm to test the benefits of those features of Lm^2. The only slight disadvantage of Lm^2 which was observed during this investigation was the lack of clear and compelling trends, compared to the classical washout algorithm, when adjusting some of the motion filter coefficients (e.g. roll-axis break frequency). This was attributed to the less direct input-output relationship in the roll-axis, due to the addition of the roll coordination feedback path. The peak in phase error of the roll-axis transfer function (Fig. 18a), caused by the use of a second-order sway-axis filter may also have played a part, since it occured at around 1 rad/s. The lack of any compelling trends when adjusting the filter coefficients may indicate that tuning of an Lm^2 algorithm could, possibly, be more challenging than for the classical washout.

It is not suggested here that the motion cues from the classical washout algorithm were poor or of limited value. On the contary, 'high' fidelity motion cues were achieved with the classical washout algorithm (see Figs. 23 and 25). On the otherhand, there are clearly improvements which could be made to the classical washout algorithm used in this experiment, for example using second-order filters rather than third-order, but these would have compromised the primary objective of repeating the previous experiment. Furthermore, on a larger platform, with a greater motion envelope, higher motion gains and lower break-frequencies could have been realized. However, the same could also be said for the Lm^2 algorithm, for example, a first-order filter could have been used in the sway-axis (as recommended in Ref. 18) and the same limitations in terms of motion gains and break frequencies applied.

It is necessary to exercise caution when drawing conclusions from the second phase of this experiment, in terms of the benefits of Lm^2 to the helicopter roll-sway task, based on the results for a single subject pilot and with practical limitations on the implementation of both algorithms (described above). Nevertheless, the pilot's strong subjective preference for the Lm^2 motion cues and the correlation between the language used by pilots to describe the motion cues with Lm^2 cannot be ignored, and warrants further detailed investigation.

Conclusions and Recommendations

The two objectives of this paper were (1) to repeat the previous roll-lateral experiment described in Ref. 15 with a different subject pilot, and (2) to examine the Lm^2 motion drive algorithm. This is the first time that the Lm^2 algorithm has been used for a helicopter roll-lateral task on a short-stroke motion platform and, to the authors' knowledge, is the first time that Lm^2 has been systematically tested in a motion fidelity experiment of this kind. The results confirm that appropriate selection of motion filter coefficients (i.e. motion tuning) is, as ever, critical to achieving high fidelity. More specifically the following conclusions are drawn:

1. Subjective ratings were taken from the Motion Fidelity Rating scale and, where ratings for both pilots are available, they were found to be in very good agreement, often being within one rating of each other (low 'interpilot' variability). This suggests that the rating scale has been interpreted and used consistently by pilots, making it a useful subjective measure.

2. The roll-axis break frequency had a dominant effect on motion fidelity during tests of the classical washout algorithm. In both the current and previous experiments a break frequency of 0.9 rad/s elicited strong pilot objections, due to mismatch (phase shift) between the vestibular and visual cues. Similar results were obtained in the current experiment for a break frequency of 0.6 rad/s although pilot objections were reduced. With break frequencies of 0.6 or 0.9 rad/s the only way to enhance simulator fidelity was to reduce the roll-axis motion gain, hence 'masking' the visual-motion mismatch.

3. Good motion cues could only be obtained by careful selection of the roll and sway-axis motion gains. This was true for both the classical washout and Lm^2 algorithms.

4. Motion cues which could be described as 'high' fidelity were obtained with both the classical washout and Lm^2 algorithms. However, the pilot who took part in this experiment preferred the motion cues from the Lm^2 algorithm, describing them as '*predictable*' and '*more like a real aircraft'*. The Lm^2 motion cues allowed him to be more aggressive during stabilisation at the target position.

5. Although it was only possible to gather the views of a single subject pilot during evaluations of the Lm^2 algorithm, the strong subjective preference and the correlation between the language used by different pilots to describe the Lm^2 motion cues cannot be ignored.

6. A further investigation should be conducted with multiple pilots, once the classical washout and Lm^2 algorithms have been optimised. Ideally, a similar roll-sway task would be conducted on a real helicopter, or very large motion simulator, to provide a database for comparision of the motion cues.

7. During a future investigation, individual elements of the Lm^2 algorithm should be tested in isolation to determine their contribution to pilots' perceptions of enhanced motion fidelity.

Acknowledgements

The first and second authors would like to thank their respective employers - BAE Systems and the Defence Science & Technology Organisation (Australia), for allowing them the opportunity to participant in this research activity. This work is contributing to GARTEUR HC/AG-21, Rotorcraft Simulation Fidelity Assessment: Predicted and Perceived Measures of Fidelity. The authors gratefully acknowledge the significant contribution made by our professional test pilots, without their involvement this work would not have been possible.

References

[1] Ashkenas, I. L., "Collected Flight and Simulation Comparisons and Considerations", AGARD Flight Mechanics Panel Symposium on 'Flight Simulation', Cambridge, UK, September-October 1985.

[2] Sinacori, J. B., "A Practical Approach to Motion Simulation", AIAA Paper 73-931, AIAA Visual and Motion Simulation Conference, Palo Alto, California, September 1973.

[3] Schroeder, J. A., Chung, W. W., and Laforce, S., "Effects of Roll and Lateral Flight Simulation Motion Gains on a Sidestep Task", American Helicopter Society 52rd Annual Forum, Virginia Beach, Virginia, April-May 1997.

[4] Reid, L. D. and Nahon, M. A., "Response of airline pilots to variations in flight simulator motion algorithms", *Journal of Aircraft*, July 1988, No. 25 (7), pp. 639-646.

[5] Stapleford, R. L., Peters, R. A., and Alex, F. R., "Experiments and a model for pilot dynamics with visual and motion inputs", 1969, NASA CR-1325.

[6] Jex, H. R., Magdaleno, R. E., and Junker, A. M., "Roll tracking effects of G-vector tilt and various types of motion washout", 1978, NASA CP-2060, pp. 463-502.

[7] Bray, R. S., "Initial operating experience with an aircraft simulator having extensive lateral motion", 1972, NASA-TM-X-62155.

[8] Van Gool, M. F. C., "Influence of motion wash-out filters on pilot tracking performance", 1978, AGARD-CP-249, AGARD Flight Mechanics Panel Specialists' Meeting on 'Piloted Aircraft Environment Simulation Techniques', Brussels, Belgium, April 1978.

[9] Bergeron, H. P., Adams, J. J., and Hurt, G. J., "The effects of motion cues and scaling on one- and two-axis compensatory control tasks", 1971, NASA TN D-6110.

[10] Shirachi, D. K., and Shirley, R. S., "Visual/motion cue mismatch in a coordinated roll maneuver", 1981, NASA-CR-152066.

[11] Sinacori, J. B., "The determination of some requirements for a helicopter flight research simulation facility", 1977, NASA-CR-152066.

[12] Mikula, J., Chung, W. W., and Tran, D., "Motion fidelity criteria for roll-lateral translational tasks", AIAA Paper 99-4329, AIAA Modeling and Simulation Technologies Conference, Portland, OR, August 1999.

[13] Chung, W. W., Robinson, D. J., Wong, J., and Tran, D., "Investigation of roll-lateral coordinated motion requirements with a conventional hexapod motion platform", AIAA Paper 98-4172, AIAA Modeling and Simulation Technologies Conference, Boston, MA, August 1998.

[14] Wiskemann, C. M., Drop, F. M., Pool, D. M., van Passen, M. M., Mulder, M., and Bulthoff, H.H., "Subjective and Objective Metrics for the Evaluation of Motion Cueing Fidelity for a Roll-Lateral Reposition Maneuver", American Helicopter Society 70th Annual Forum, Montreal, Quebec, May 2014.

[15] Hodge, S. J., Perfect, P., Padfield, G. D., and White, M. D, "Optimising the roll-sway motion cues available from a short-stroke hexapod motion platform", *The Aeronautical Journal*, January 2015, Vol. 119 (1211), pp. 23-44.

[16] Nahon, M. A., and Reid, L. D., "Simulator Motion-Drive Algorithms: A Designers Perspective", Journal of Guidance and Control, March-April 1990, 13 (2), pp. 356-362.

[17] Grant, P. R., and Reid, L. D., "Motion Washout Filter Tuning: Rules and Requirements", Journal of Aircraft, March-April 1997, No. 2 (34), pp. 145-151.

[18] Van Biervliet, F., "Lm^2 – Lateral Manoeuvring Motion", RAeS Flight Simulation Group conference 'Expanding Horizons: Technology Advances in Flight Simulation", June 2008, London, UK.

[19] Learmount, D., "Sabena shakes up simulation", Flight International, March 2007.

[20] Learmount, D., "USAF chooses Lm2 simulator motion modifier for KC-135 training", Flight International, July 2014.

[21] White, M. D., Perfect, P., Padfield, G. D., Gubbels, A. W., and Berryman, A., "Acceptance and Testing of a Rotorcraft Flight Simulator for Research and Teaching: The Importance of Unified Metrics", 35th European Rotorcraft Forum, September 2009, Hamburg, Germany.

[22] Fielding, C., and Southworth, M. R., "Piloted simulation developments of STOVL aircraft handling qualities, AIAA Paper 2001-4263, AIAA Guidance, Navigation and Control Conference, August 2001, Montreal, Canada.

[23] Hodge, S. J., Perfect, P., Padfield, G. D., and White, M. D., "Optimising the cues available from a short-stroke hexapod platform", American Helicopter Society 67th Annual Forum, Virginia Beach, VA, May 2011.

[24] Wilson, D. J., and Riley, D. R., "Cooper-Harper Pilot Rating Variability", AIAA 89-2258, AIAA Atmospheric Flight Mechanics Conference, Boston, MA, August 1989.